# Amplification of soft x rays in Ne-like germanium ions created by 0.53-$\mu$m laser light

D. Naccache, A. Decoster, S. Jacquemot, and M. Louis-Jacquet
*Commissariat à l'Énergie Atomique, Centre d'Études de Limeil-Valenton, 94195 Villeneuve-Saint-Georges CEDEX, France*

C. J. Keane, B. J. MacGowan, and D. L. Matthews
*Lawrence Livermore National Laboratory, University of California, Livermore, California 94550*
(Received 17 November 1989)

We have performed experiments on germanium plasma irradiated with 0.53-$\mu$m laser light. A soft-x-ray amplification was observed. 2- and 2.4-cm$^{-1}$ gains were measured for the two brightest lasing lines at 232.2 and 236.2 Å. A temporal analysis of lasing lines and gain is reported. Simulations by a series of computer programs compared favorably with the measured values and contributed to the clarification of some experimental results.

## I. INTRODUCTION

A wide variety of experiments have been carried out at Centre d'Études de Limeil-Valenton, France, with the Phebus facility delivering 0.53- and 0.35-$\mu$m laser light to investigate the x-ray laser physics in the neonlike excitation scheme. The purpose is to optimize the amplification in this system by varying both the nature and thickness of targets and laser irradiation. With this aim in view we did many experiments with selenium, molybdenum, strontium, and germanium. Gains had been already measured in Se,[1,2] and in Mo,[3] but the first observation in Sr was achieved in CEL-V.[4] Lasing in thick germanium targets had been demonstrated with 1.06-$\mu$m wavelength at Naval Research Laboratory (NRL),[5] at Rutherford Appleton Laboratory (RAL),[6] and in preliminary experiments on thin foils at CEL-V.[7] This element was chosen by the three laboratories because it was compatible with a lower-power driving laser (Pharos laser at NRL and Octal laser at CEL-V).

In this paper, we present studies on germanium which have been conducted with Phebus 0.53-$\mu$m laser light. Germanium was chosen, first to compare with 1.06-$\mu$m wavelength results, and also to get more data about the way gain scales with the target atomic number. In a typical experiment, the amplifying medium is a thin foil, which is vaporized to produce a fairly uniform plasma with suitable conditions to provide population inversions between $3p$ and $3s$ levels. The large electron density scale length within the plasma allows the x rays to propagate down the length of the amplifier without too much refraction, so that a large gain-length product is achieved. Figure 1 is a simplified level diagram showing the main lasing transitions. Ions are excited by electrons towards upper levels of inversion by collisional excitation from the ground state, particularly for the $(3p\text{-}3s)_{J=0-1}$ transitions. In addition, a combination of dielectronic recombination from F-like ions and cascades from higher $n$ states and $3d$ levels contribute also to populate the $(3p-3s)_{J=2-1}$ upper levels. The $2p^5 3s$ shell decays to the $2p^6$ ground state by fast dipole transitions, while the $2p^5 3p$ states can radiate only by much slower quadrupole transitions, thus maintaining the population inversion. As in previous results for Se,[1] and Mo,[3] a higher gain in Ge is observed from $J=2$-1 lasing lines at 236.25 and 232.21 Å than from the $J=0$-1 line at 196.1 Å.

## II. EXPERIMENTAL SETUP

For our study, the two beams of the Nd-glass laser Phebus[8] delivered up to 1500 J per chain of 0.53-$\mu$m light in a 500- or 850-ps pulse. For each beam a combination of a spherical lens and a pair of cylindrical lenses provid-

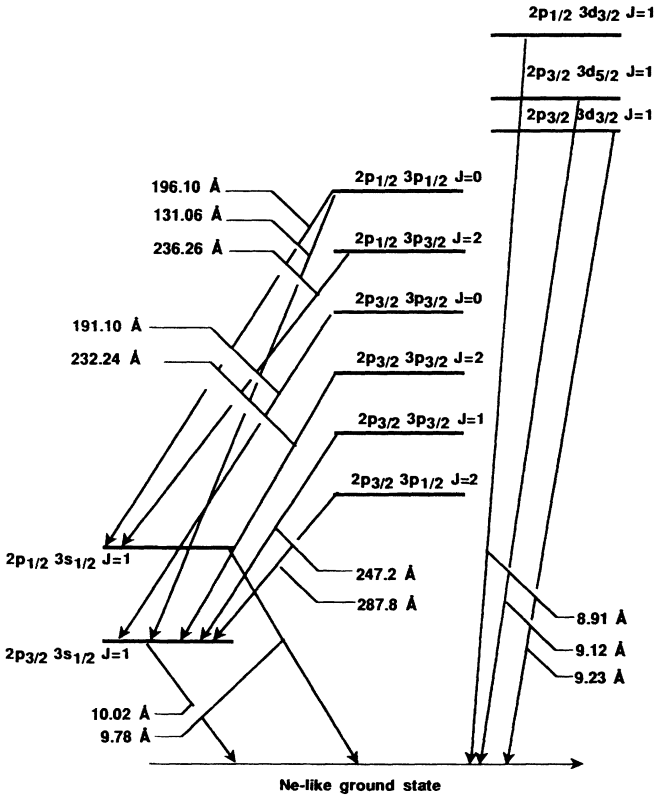


FIG. 1. Ne-like germanium-level diagram.

 

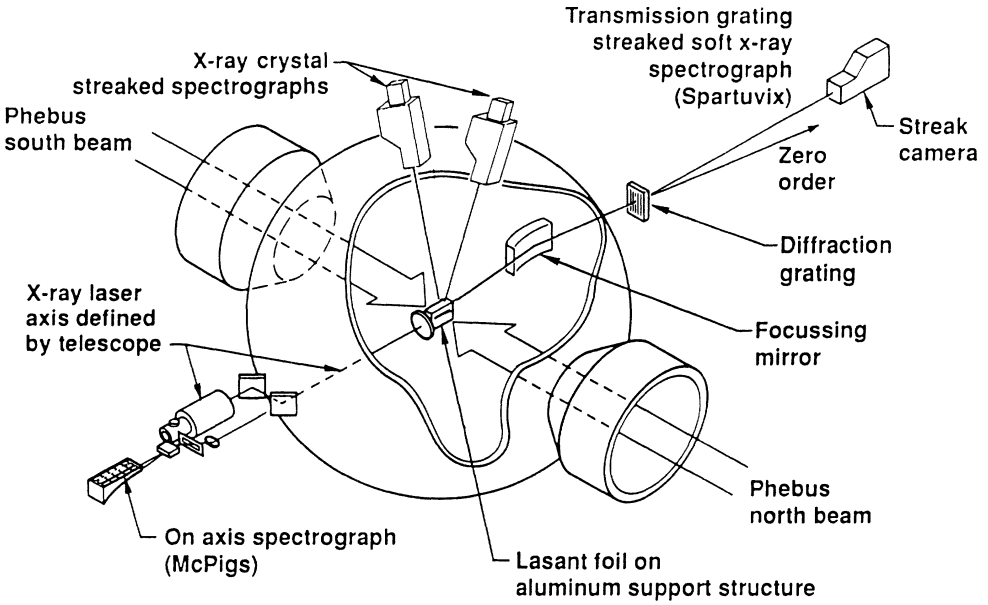


FIG. 2. Experimental setup.

ed a line focus continuously variable in length up to 2.7 cm. The two beams were superimposed on the target with a colinear accuracy of $\pm 1.5$ mrad. The line focus width was between 200 and 300 $\mu$m. Figure 2 shows a schematic view of the target chamber with the location of the diagnostics. The two main diagnostics used to record spectra and to measure gains were the reflection grating soft-x-ray McPigs spectrograph, and the transmission grating streaked soft-x-ray Spartuvix spectrograph. The former provides high-resolution (0.1–0.2 Å) time gated spectra, while the Spartuvix spectrograph yields continuous time resolution of soft-x-ray emission with less spectral resolution (0.7 Å). A complete description of these two spectrographs has been made previously.[9,10] Both instruments are collinear with the direction of x-ray laser axial emission within an accuracy of 1.5 mrad. The common axis for the target and the two spectrographs was defined with the alignment system bound up with the McPigs spectrograph.[3] In order to characterize both the x-ray radiation (3-2 emission) and the plasma ionization kinetics, a pair of streaked x-ray crystal spectrographs was positioned off the x-ray laser axis.

## III. EXPERIMENTS

The shots were carried out on two types of targets: slabs and thin films. The latter consisted of Formvar foils of areal density 15 $\mu$g/cm$^2$ overcoated with 27 or 34 $\mu$g/cm$^2$ of germanium. 27-$\mu$g/cm$^2$ targets of 0.8-, 1.7-, and 2.2-cm lengths were used at $6\times10^{13}$ W/cm$^2$ total irradiance; the thicker 34-$\mu$g/cm$^2$ foils had only two lengths, 0.8 and 2.2 cm, but were studied at $2\times10^{13}$ and $6\times10^{13}$ W/cm$^2$. In addition, two long-slab targets were irradiated (at $6\times10^{13}$ W/cm$^2$) to compare with 1.06-$\mu$m results.[5]

The two expected $(3p\text{-}3s)_{J=2-1}$ lines, whose wavelengths are 232.21 and 236.25 Å, were observed to be the brightest lines in the different spectra in all cases (Fig. 3). Two other lasing lines were identifiable, the $J=0$-1 transition at 196.1 Å (analogous to the 182.4-Å one in Se), and the $J=2$-1 transition at 287.8 Å (262.94 Å in Se). The $J=1$-1 transition at 247.2 Å (220.4 Å in Se) was ob-

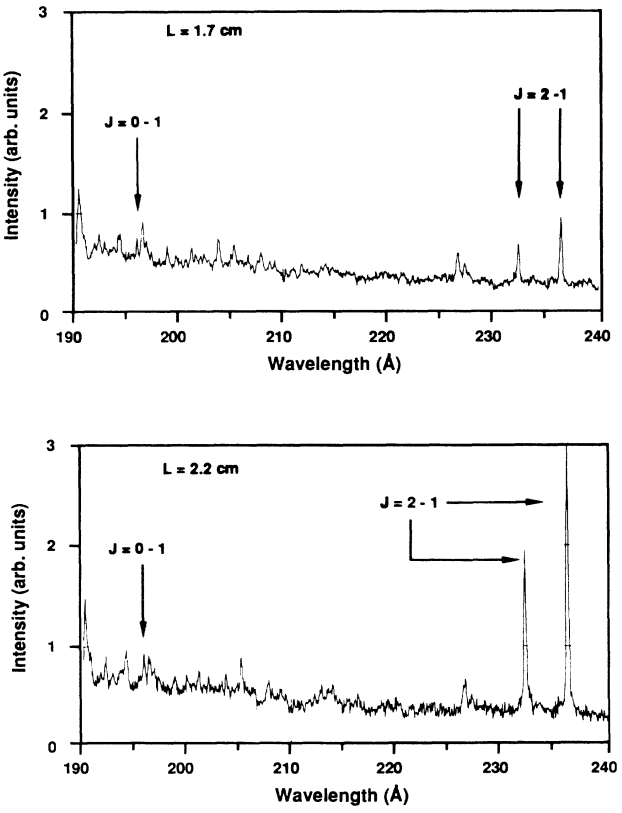


FIG. 3. Neonlike Ge spectra recorded for 1.7- and 2.2-cm plasma lengths, showing the amplification of lasing lines.

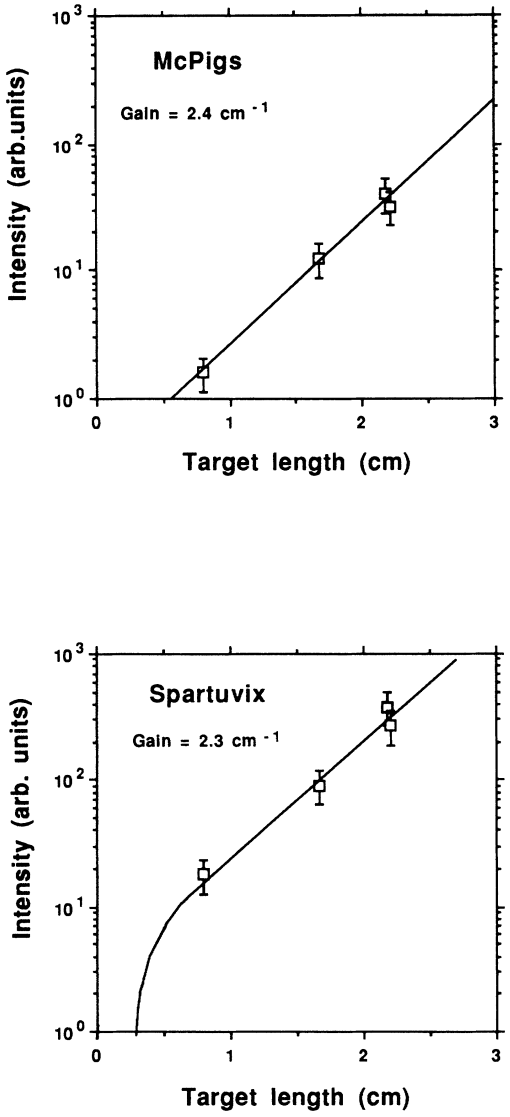


FIG. 4. Determination of gain for the 236.2-Å line.

served on a few shots only, and its intensity was too low to deduce a gain. By analogy with previous results in Ne-like ions, we looked for the $(3p_{3/2}\text{-}3s_{1/2})_{J=0-1}$ line calculated at 191.1 Å;[11] this line is equivalent to the 104.6-Å one in Mo, for which a noteworthy gain had been determined;[3] unfortunately, this line in germanium is blended with a strong Na-like line at 190.6 Å.[12] The $(3p_{1/2}\text{-}3s_{1/2})_{J=0-1}$ line at 131.06 Å was identified on one shot (27-$\mu$g/cm$^2$ target of 2.2-cm length at $6\times10^{13}$-W/cm$^2$ total irradiance); this transition has the same upper state as the 196.1-Å line and the same lower state as the 191.1-Å line.

In addition to the lasing lines, many transitions from germanium in different ionization stages, such as F-, Ne-, Na-, and Mg-like stages, are present in spectra, as well as numerous lines of carbon (C V and C VI) and oxygen (O I, O VI, and O VIII). These elements are components of the target substrate (Formvar); oxygen comes also from germanium oxidation. These identifications were made by comparison of McPigs spectra with a list of calculated and measured line values.[7,11–15] In particular, the strong optically thick $3s$-$3p$ and $3p$-$3d$ Na-like lines[12] provided a check of the wavelength scale accuracy.

In this type of experiment, the gain on a given transition is determined by looking at the variation of the line intensity with the target length. Measurements of gain were performed using both McPigs and Spartuvix spectrographs. The gain curves of the 236.2-Å line from 27-$\mu$g/cm$^2$ targets for the two spectrographs are shown in Fig. 4.

The solid line represents a best fit of the gain scaling formula

$$[\exp(gl)-1]^{3/2}/[gl\exp(gl)]^{1/2}$$

for amplified spontaneous emission through a plasma length $l$, with a gain coefficient $g$ at the line center. These experimental values are shown in Table I for the two kinds of thin targets.

The 196.1-Å line was seen with the Spartuvix spectro-

TABLE I. Gains at $6\times10^{13}$ W/cm$^2$ irradiance (experimental uncertainties are of the order of $\pm0.2$ cm$^{-1}$).

| Areal density ($\mu$g/cm$^2$) | Lasing line | | Gain (cm$^{-1}$) | | |
|---|---|---|---|---|---|
| | | (Å) | McPigs | Spartuvix | Theory |
| 27 | $J=0$-1 | 196.1 | 0.96 | | |
| | $J=2$-1 | 232.2 | 2. | 2.1 | 2.2 |
| | | 236.2 | 2.4 | 2.3 | 1.8 |
| | | 287.8 | 1.8 | | 2.1 |
| | $J=1$-1 | 247.2 | | | 1. |
| 34 | $J=0$-1 | 196.1 | | | |
| | $J=2$-1 | 232.2 | 2.1 | 2. | 1.7 |
| | | 236.2 | 2.2 | 1.7 | 1.3 |
| | | 287.8 | 1.8 | | 1.7 |
| | $J=1$-1 | 247.2 | | | 0.75 |

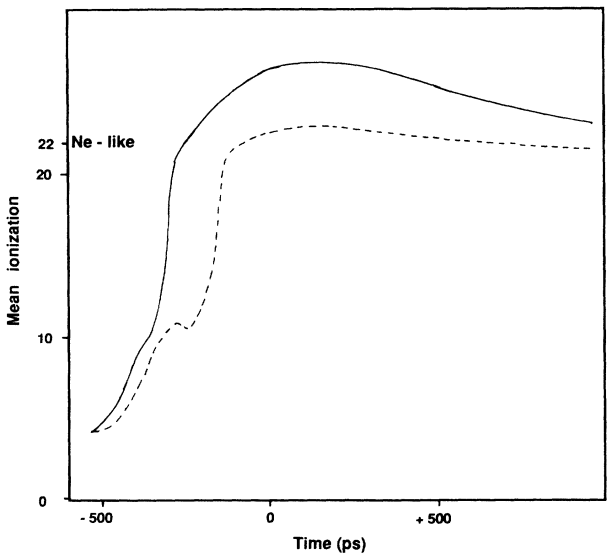


FIG. 5. Mean ionization value at the center of a 34-$\mu$g/cm$^2$ Ge target irradiated at $6\times10^{13}$ W/cm$^2$ (——), and $2\times10^{13}$ W/cm$^2$ (— — —). Time 0 is at the maximum of the laser pulse.

graph on a few shots only, and in all cases its intensity was too low to provide a reliable gain determination. The $J=2$-1 line at 287.8 Å is out of range for the Spartuvix spectrograph. As we can see in Table I, a similar gain was found for the two thin target types, but four experimental points were used in the 27-$\mu$g/cm$^2$ case and two points in the other case; if two points only had been taken for the thinner targets, a higher gain would have been deduced. At low intensity ($2\times10^{13}$ W/cm$^2$) with the thicker 34-$\mu$g/cm$^2$ targets, no gain could be determined because of the weak level of emission at shorter lengths.

## IV. GAIN DISCUSSION

Simulations of the x-ray laser effect were done, as for other Ne-like cases, by a series of computer programs. The one-dimensional hydrodynamical code CHIVAS describes a variable ionization (either local thermodynamic equilibrium or coronal, whichever gives the lowest ionization value) perfect gas with laser absorption and energy transport. From the density and temperature profiles thus given, the detailed kinetics code LASIX determines ionization balance and atomic populations, yielding a raw local value of the gain of lasing transitions. A correction for refraction of x-ray laser light is provided by the ray-trace and amplification code OPTIQX.

The hydrocode parameters were (i) classical inverse Bremsstrahlung absorption with Skupsky correction[16] and a $0.8\times$ factor, and Langdon effect;[17] (ii) an energy dump at critical density (17% for 0.53-$\mu$m laser light, 30% for 1.06 $\mu$m); (iii) an $f=0.1$ harmonic flux limiter at 0.53 $\mu$m ($f=0.06$ at 1.06 $\mu$m).

The resulting theoretical gain values are shown in Table I for the thin-film targets at $6\times10^{13}$-W/cm$^2$ irradiance. The agreement with experiment is satisfactory; we know, however, that the theoretical gains of $J=0$-1 lines are unreliable, as in other Ne-like scheme cases. The weak x-ray emission of 34-$\mu$g/cm$^2$ targets irradiated at $2\times10^{13}$ W/cm$^2$ is easily explained by a much lower temperature (600-eV peak value instead of 1000-eV in other cases): the Ne-like and F-like ionization stages are reached too late, near the maximum of the laser pulse (Fig. 5), while the optimum time would be about 100 ps before.

The refraction code OPTIQX works in two stages. First, at a given time, a sampling of rays arriving on a given point of the detector is traced through the plasma. For example, Fig. 6 shows an electron density profile and a corresponding ray trace for one of our targets; every ray in Fig. 6(b) reaches the center of the detector, 70 cm farther on the right. All rays are represented here as if they were equal, but of course they carry different amounts of x-ray laser flux (in the case of this figure, the rays running through the plastic do not carry any). A second stage is thus the calculation of the amplification along each ray using gain and source term profiles from LASIX. Summing up the contributions of all rays and all points on the detector, an x-ray flux is obtained. Repeating this last stage for different plasma lengths is a simulation of the experimental way of determining the gain. It is more realistic than the simpler London model,[18] which can be used only for the ideal case of a parabolic electron density profile.

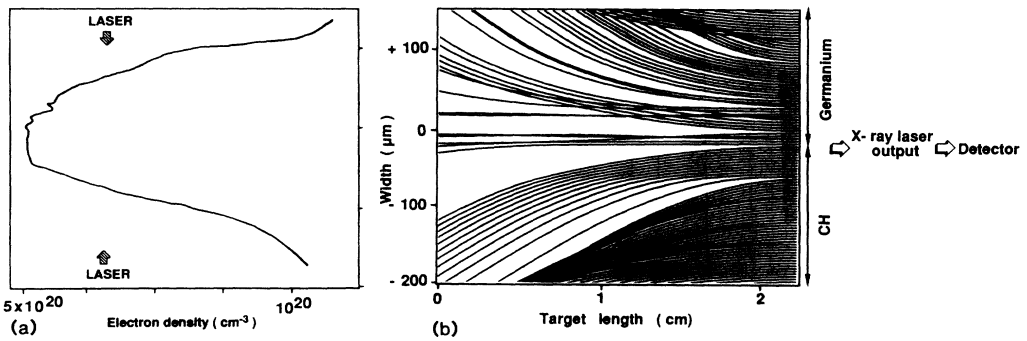


FIG. 6. Ray tracing of a $J=2$-1 x-ray laser line: thin foil at 0.53 $\mu$m (b). Irradiation conditions are $6\times10^{13}$ W/cm$^2$ and 500 ps FWHM. The ray trace is made 70 ps before the maximum of the laser pulse. The corresponding electron density profile is shown in (a).

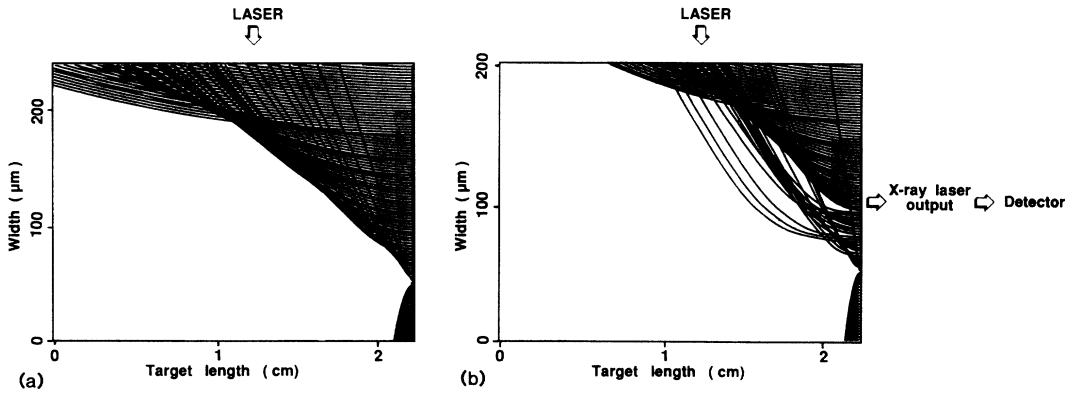


FIG. 7. Ray tracing of a $J=2$-1 x-ray laser line: slab targets at (a) 1.06 $\mu$m and (b) 0.53 $\mu$m. Irradiation conditions are $6\times10^{13}$ W/cm$^2$ and 500 ps FWHM. The ray trace is made 70 ps before the maximum of the laser pulse.

The comparison of the massive targets experiments performed with 1.06-$\mu$m driving laser light at NRL or recently at RAL, with ours carried out with 0.53-$\mu$m-thick targets and thin foils illustrates the importance of refraction in x-ray laser observation. While in the NRL and Rutherford, noteworthy gain had been measured on bulk targets, the weak level of lasing lines made gain determination impossible in our studies. Compared to 1.06-$\mu$m simulations, the second-harmonic ones showed a steeper electron density gradient, peaking at much higher values. Then, as seen in Fig. 7, the x-ray curvature is thus increased, so that the laser emission is not able to propagate down the entire length of the plasma, and a lower intensity is measured. In addition, we note that the main spectrograph, which was used to detect the x-ray laser, was positioned in NRL experiments close to the target (4 cm), and the RAL diagnostic could be moved off the target axis. On the contrary, our spectrograph was located on the target axis and relatively farther (about 150 cm). Figure 8 shows a simulation of the x rays received on the detector at 150 cm: the beam is well off axis, so that our spectrograph is not able to record all the x rays. The NRL detector and ours are in a similar geometrical situation, but ours obviously receives a lower flux, whence a low signal-to-noise ratio. So, in our studies, both the use of 0.53-$\mu$m laser light and the diagnostic location are unfavorable to observe an x-ray laser emission from a bulk target.

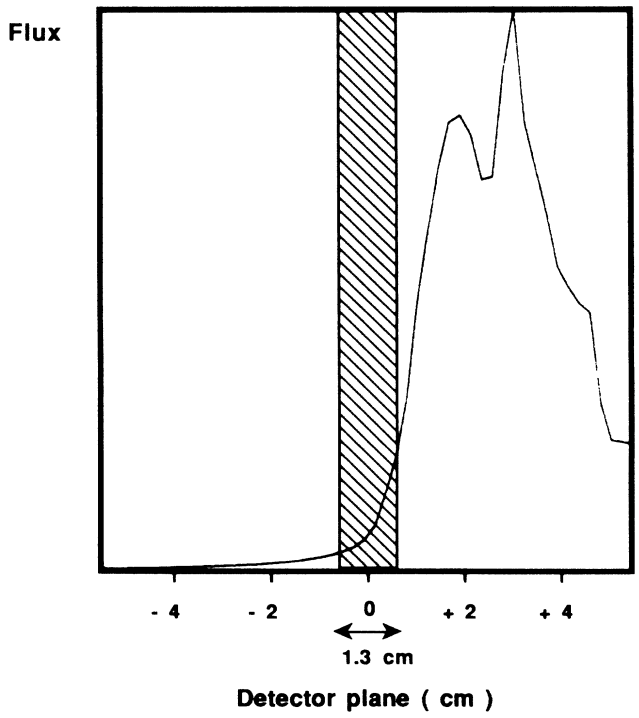


FIG. 8. Simulation of the x-ray flux coming from a thick target, as seen at the detector location (at a 150-cm distance). Only the hatched part is actually recorded through the 1.3-cm aperture spectrograph. Experimental conditions: 0.53-$\mu$m laser light, 2.2-cm-long plasma.

Examination of Figs. 6(b) and 7(b), which are simulations at 0.53 $\mu$m, respectively, for slab and thin targets, illustrates our results at this wavelength: exploding foils, unlike thick targets, provide an underdense plasma where the electron density gradient established is relatively smooth, and refraction effects play a smaller part. We note also that the previous 1.06-$\mu$m thin foils experiments undertaken at CEL-V (Ref. 7) gave gains similar to the ones of Table I. To summarize, the refraction is as expected disadvantageous with massive targets and when the driving laser wavelength decreases.

## V. TIME HISTORY

Spartuvix spectrograph data allow us to draw the gain evolution as a function of time. During our experiments, the x-ray streak camera integral with the spectrograph was not equipped with an absolute time reference correlated with the laser pulse. So, we chose as timing reference the beginning of the time intensity curves of lasing lines. Then, only the gain curve form is meaningful, since the time acquisitions are not synchronized with the driving laser. Figure 9 shows the measured time history of

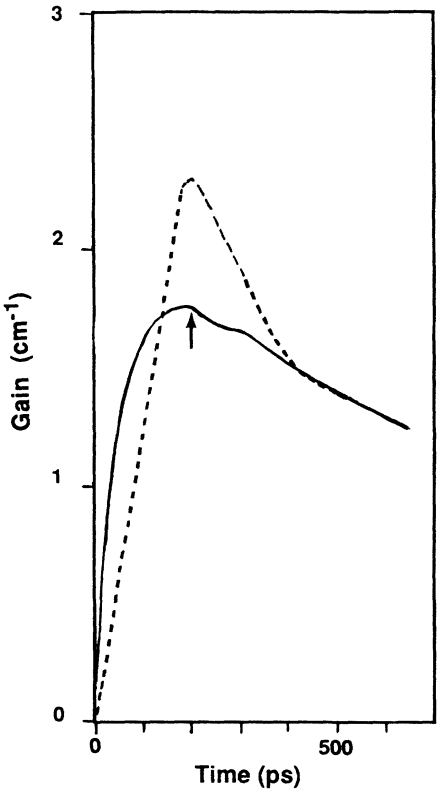


FIG. 9. Gain time history of the 236.2-Å line: — — —, experimental; ——, theoretical.

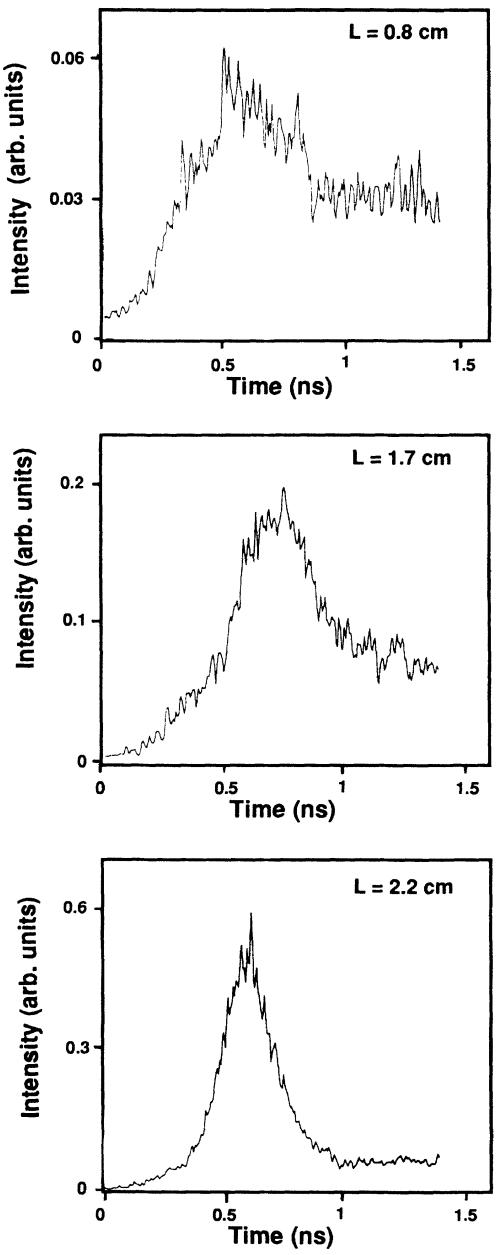


FIG. 10. Time history of the 236.2-Å line.

the gain in the 236.2-Å lasing line case; for each time we calculated the gain with three 27-$\mu$g/cm$^2$ target lengths (0.8, 1.7, and 2.2 cm) and the laser pulse was a Gaussian of 500 ps full width at half maximum (FWHM). Figure 9 also shows the theoretical gain history for the same line, with an arrow pointing to the time of the maximum of the laser pulse. The gain grows up quickly to the maximum and decreases progressively. This behavior is connected to the fact that in this type of study the target explodes during the *rising* time of the laser pulse; the plasma conditions are then optimum, insofar as being optimized for production of the population inversion by collisional excitation.

The experimental time history of the lasing lines is provided by the Spartuvix spectrograph, which gives continuous time resolution of the soft-x-ray emission; the time resolution is about 30 ps. This type of spectrograph allows us to evaluate the duration of the population inversion. We observe a reduction of the duration FWHM of x-ray laser emission when the target length increases. For the 27-$\mu$g/cm$^2$ case, the 236.2-Å line lasts 560 ps for 0.8-cm-long targets, 450 ps for 1.7 cm, and 250 ps for 2.2 cm (Fig. 10); since the intensity is an exponential expression of $gl$ ($g$, gain; $l$, target length), when $gl$ increases, the full width at half maximum of the intensity curve versus time decreases. The temporal profiles of the lines from the different ionization stages give interesting information about the plasma evolution; for instance, the longer time duration of the Na-like Ge line at 226.5 Å compared to the Ne-like x-ray laser line at 236.2 Å: 1.1 ns instead of 0.45 ns for 1.7-cm-long targets.

## VI. CONCLUSION

X-ray laser experiments on germanium with 0.53-$\mu$m laser light have demonstrated some potentially interesting scaling as a function of the atomic number of the las-

ing element. These gain measurements supplement the data obtained with other Ne-like ions: Se, Mo, and Sr.

The results from 1.06- and 0.53-$\mu$m driving laser light, and thick and thin targets, show the prominence of refraction effects in the plasma. The geometry and location of the spectrograph were found critical in some cases. The temporal analysis of the phenomena from the time-resolved spectra (x-ray and soft-x-ray) provides information about the evolution of plasma parameters and about gain production.

## ACKNOWLEDGMENTS

We would like to express our appreciation to G. Thiell and the Phebus operation crew for their outstanding work during the entire series of joint Lawrence Livermore National Laboratory (LLNL)-CEL-V x-ray laser experiments. Also we thank J. L. Bourgade and P. Combis for their help with the spectrgraphs, the target crew for their efforts in target preparation, and the LLNL personnel for their contributions.

[1]D. L. Matthews *et al.*, J. Opt. Soc. Am. B **4**, 575 (1986).

[2]B. J. MacGowan *et al.*, in *SPIE Proceedings on Multilayer Structures and Laboratory X-ray Laser Research,* edited by N. Ceglio and P. Dhez (SPIE, The International Society for Optical Engineering, Washington, D.C., 1986), Vol. 688, p. 36; Opt. Instrum. Eng. **688** (1986).

[3]B. J. MacGowan *et al.*, J. Appl. Phys. **61**, 5243 (1987).

[4]C. J. Kean *et al.*, in *OSA Proceedings on Short Wavelength Coherent Radiation: Generation and Applications,* edited by R. Falcon and J. Kirz (Optical Society of America, Washington, D.C., 1989), Vol. 2.

[5]T. N. Lee, E. A. McLean, and R. C. Elton, Phys. Rev. Lett. **59**, 1185 (1987).

[6]C. L. S. Lewis *et al.*, Rutherford Appleton Laboratory Annual Laser Report RAL-89-045 (1989) (unpublished), p. 13.

[7]M. Louis-Jacquet *et al.*, C. R. Acad. Sci. **306**, 867 (1987).

[8]G. Thiell *et al.*, Laser Part. Beams **6**, 93 (1988).

[9]M. J. Eckart and N. M. Ceglio, in Lawrence Livermore Laboratory Report No. UCRL-52000-85-11, p. 25, 1985 (unpublished).

[10]J. L. Bourgade *et al.*, Rev. Sci. Instrum. **59**, 1840 (1988).

[11]J. A. Cogordan and S. Lunell, Phys. Scr. **33**, 406 (1985).

[12]J. Reader *et al.*, J. Opt. Soc. Am. B **4**, 1821 (1987).

[13]J. H. Davé *et al.*, J. Opt. Soc. Am. B **4**, 635 (1987).

[14]W. E. Behring *et al.*, J. Opt. Soc. Am. **66**, 376 (1976).

[15]R. L. Kelly, J. Phys. Chem. Ref. Data **16**, Suppl. No. 1 (1987).

[16]S. Skupsky, Phys. Rev. A **36**, 5701 (1987).

[17]A. B. Langdon, Phys. Rev. Lett. **44**, 575 (1980).

[18]R. A. London, Phys. Fluids **31**, 184 (1988).